View metadata, citation and similar papers at core.ac.uk
brought to you by CORE
provided by Repositorio da Producao Cientifica e Intelectual da Unicamp

Growth and characterization of GaAlAs/GaAs and GaInAs/InP structures: The effect of a pulse metalorganic flow

M. Sacilotti, L. Horiuchi, J. Decobert, M. J. Brasil, L. P. Cardoso, P. Ossart, and J. D. Ganière

Citation: Journal of Applied Physics **71**, 179 (1992); doi: 10.1063/1.350734
View online: http://dx.doi.org/10.1063/1.350734
View Table of Contents: http://scitation.aip.org/content/aip/journal/jap/71/1?ver=pdfcov
Published by the AIP Publishing

Articles you may be interested in
Suppression of wavy growth in metalorganic vapor phase epitaxy grown GaInAs/InP superlattices
Appl. Phys. Lett. **69**, 2101 (1996); 10.1063/1.116893

Interfacial properties of very thin GaInAs/InP quantum well structures grown by metalorganic vapor phase epitaxy
J. Appl. Phys. **71**, 3300 (1992); 10.1063/1.350949

Structural characterization of very thin GaInAs/InP quantum wells grown by atmospheric pressure organometallic vapor-phase epitaxy
J. Appl. Phys. **67**, 563 (1990); 10.1063/1.345193

GaInAs-InP multiquantum well structures grown by metalorganic gas phase epitaxy with adducts
Appl. Phys. Lett. **48**, 911 (1986); 10.1063/1.96655

Growth of GaInAs-InP multiquantum wells on garnet (GGG=Gd3Ga5O1 2) substrate by metalorganic chemical vapor deposition
J. Appl. Phys. **59**, 2261 (1986); 10.1063/1.336374

[This article is copyrighted as indicated in the article. Reuse of AIP content is subject to the terms at: http://scitation.aip.org/termsconditions. Downloaded to] IP: 143.106.108.136 On: Tue, 23 Jun 2015 18:19:15

Growth and characterization of GaAlAs/GaAs and GaInAs/InP structures: The effect of a pulse metalorganic flow

M. Sacilotti, L. Horiuchi, and J. Decobert
CPqD-Telebrás, Caixa Postal 1579, 13083 Campinas, SP Brazil

M. J. Brasil and L. P. Cardoso
Instituto de Fisica - UNICAMP, CP 6165, 13081 Campinas, SP Brazil

P. Ossart
CNET - 196 Avenue Henri Ravera, 92220 Bagneux, France

J. D. Ganière
Ecole Polytechnique Fédérale de Lausanne, Departement de Physique, CH-1015 Lausanne, Switzerland

(Received 3 April 1991; accepted for publication 24 September 1991)

GaAlAs/GaAs and GaInAs/InP thick layers, single and multiple quantum wells were grown by atmospheric pressure metalorganic vapor phase epitaxy. Auger electron spectroscopy, wedge transmission electron microscopy, x-ray diffraction, low-temperature photoluminescence, and scanning electron microscopy were used to analyze the crystal quality. These analysis techniques show that layers grown using high vapor pressure metalorganic sources present fluctuations in the ternary alloy composition. We propose that these fluctuations are due to the pulse character of the high vapor pressure metalorganic flow. Bubbling experiments were performed to show the relationship between ternary layer composition fluctuation and the pulse character of the metalorganic flow. High vapor pressure metalorganic source like trimethylgallium presents tens of Angströms growth rate per pulse or bubble whereas a low vapor pressure source like triethylgallium presents few Angströms growth rate per bubble.

I. INTRODUCTION

Metalorganic vapor phase epitaxy (MOVPE) and molecular-beam epitaxy (MBE) are the most powerful techniques to produce thin layers and abrupt heterointerfaces. Both techniques have been extensively utilized to grow quantum wells (QWs), superlattices, quantum wires, and to fill up atomic steps in a controlled way.[1–4] MBE has been recognized to give the highest two-dimensional (2D) electron gas mobility and the sharpest photoluminescence lines for GaAlAs/GaAs quantum structures.[5–10] Nevertheless, both techniques are able to produce high quality III-V bulk (thick layers) materials, with slightly better results for the MOVPE technique for indium-based materials.[11–19]

Possible explanations for the MOVPE lower 2D mobility, for the growth of heterostructures, are related to: (i) interface abruptness and homogeneity of the alloy composition, (ii) contamination of the interface and alloy by high vapor pressure impurities like oxygen and silicon from the system and sources, (iii) barrier fluctuation and asymmetry due to the reactor and bypass lines pressure imbalance and due to a nonuniform metalorganic (MO) flow, and (iv) no gas phase draining due to dead space volumes or higher vapor pressure constituents, intrinsic to the MOVPE technique.

This paper describes the atmospheric pressure (AP) MOVPE growth and characterization of GaAlAs/GaAs and GaInAs/InP layers. We show that ternary layers present composition fluctuations along the growth direction due to the pulse character of the metalorganic flow, which can also affect the interface abruptness. To our knowledge, this is the first time that the interface abruptness is correlated to the pulse character of the MO flow. These results are very important for those working with atmospheric pressure reactors.

High-resolution Auger electron spectroscopy (AES) and wedge transmission electron microscopy (WTEM) are used to analyze the composition ternary layer fluctuation. Low-temperature photoluminescence (PL), x-ray diffraction (XRD), and scanning electron microscopy (SEM) are used to analyze the crystal quality and to support the AES and WTEM results.

II. EXPERIMENTAL

A. The MOVPE system

The MOVPE system is a home-made one, operating at atmospheric pressure, rf induction heated and equipped with a Thomas Swan fast delivering switching manifold. The quartz reactor has a square cross section with a 9° cone-shape entrance, without dead space volume to avoid vortices and memory effects, as shown in Fig. 1. High gas velocity (32 to 64 cm/s), due to the reactor small cross section and to the hydrogen carrier gas high flow (5–10 slm), allows fast gas phase switching. This carrier gas velocity approaches to the low pressure reactor regime ($\sim$100 cm/s). At these conditions, ternary and quaternary layers can be grown lattice matched to the substrate for more than 15 cm^2, without susceptor rotation, low pressure, and water cooling. All the MO lines have a 100-sccm hydrogen dilution line connected to allow high gas speed within them. The reactor exaust line has mechanical and

 0021-8979/92/130179-08$04.00 © 1992 American Institute of Physics

[This article is copyrighted as indicated in the article. Reuse of AIP content is subject to the terms at: http://scitation.aip.org/termsconditions. Downloaded to] IP: 143.106.108.136 On: Tue, 23 Jun 2015 18:19:15

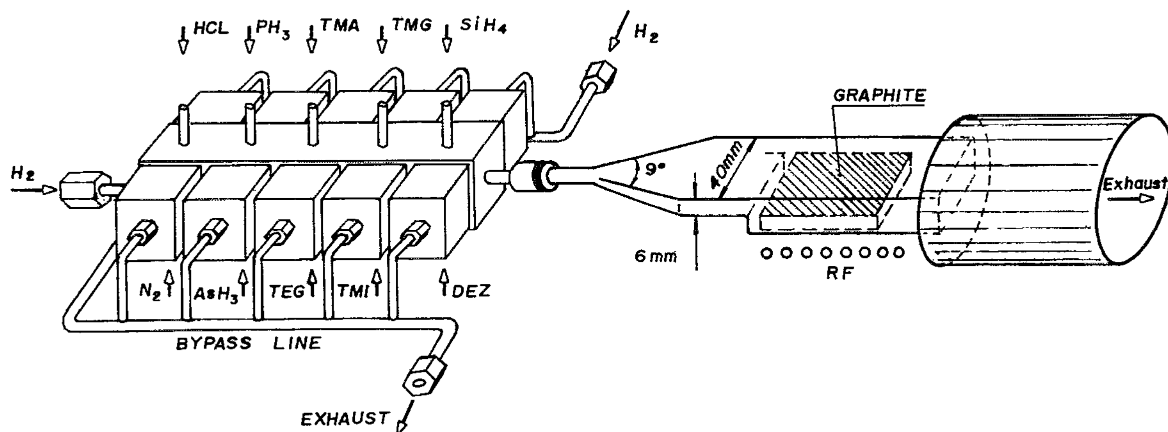

FIG. 1. Schematic representation of the APMOVPE reactor cell and the Thomas Swan manifold with the MO and hydrides sources. The graphite susceptor is heated by radio frequency (rf).

chemical cleaning procedures: glass wool, molecular sieve, mineral oil, HNO_3, and water, to avoid air pollution. The MO commercial sources utilized are: TMG, TMA, TEG, TMI, and DEZ from Alfa Ventron. The hydrides commercial sources are AsH_3, PH_3, SiH_4, and HCl from Air Liquide.

B. The layers structures

$Ga_{1-x}Al_xAs$ ($0<x<0.5$) and $Ga_{1-y}In_yAs$ ($y\sim0.53$) thick and thin layers were grown on [100] GaAs and InP substrates, respectively. Single quantum well (SQW) or a series of QW (MQW), in which the growth time was varied, were grown to check the reactor conditions and their influence on the interface abruptness. Growth rate velocities are taken from thick layer measurements and are 5–10 Å/s for GaAlAs/GaAs and 4–8 Å/s for GaInAs. Bulk GaAs, InP, and $Ga_{0.47}In_{0.53}As$ layers exhibited 77 K Hall mobilities and donors concentration of 94 000 cm^2/V s and 2×10^{14} cm^{-3}, 95 000 cm^2/V s and 1×10^{14} cm^{-3} and 56 000 cm^2/V s and 2×10^{15} cm^{-3}, respectively. The electrical characteristic of GaAlAs presents an increasing intrinsic donor density (n) as the Al composition increases for both TMG and TEG sources. For the TMG source n increases from 2–3 $\times10^{14}$ to 7×10^{15} cm^{-3} and for the TEG source n increases from 3–4 $\times10^{15}$ to 5×10^{16} cm^{-3}, when Al increases from 0% to 35%.

III. CHARACTERIZATION

A. Auger spectroscopy

Auger measurements were performed in a Jeol Scanning Auger Electron Microprobe JAMP 10S, coupled with Ar ion sputtering. The ion energy was 1 keV for current density of 5×10^{-8} A/cm^2 and the erosion rate was 15 Å/min. Measurements were done at every 30 s (7.5 Å). The ion beam makes an angle of 37° relative to the sample surface. The analyzed surface by the ion beam was 2×2 mm^2. The Al, Ga, and In lines followed were 1396, 1070, and 404 eV, respectively. During data acquisition the ion erosion was stopped.

B. Wedge transmission electron microscopy

Observations by transmission electron microscopy of cleaved samples were performed on GaAlAs/GaAs QW. This technique offers some unique advantages in terms of chemical composition information and thickness determination.[20,21] The edge of the specimen, which is cleaved along 110 planes, is transparent to the electrons and observed along [100] zone axis. Due to the well defined geometry of the specimen, the equal thickness fringes pattern can be unambiguously interpreted in terms of chemical composition fluctuations. Abrupt discontinuities in the fringes pattern are associated with abrupt interfaces between two homogeneous materials, while continuous changes in the fringes profile indicate a slow variation in the chemical composition. In particular, if the interfaces are accurately parallel to the observation direction, gradient of composition on the nanometer scale can be detected.[20,21]

C. Photoluminescence spectroscopy

Photoluminescence measurements were performed at 77 and 2 K using a Ar-ion laser as excitation source. The power density employed was 100 mW/cm^2 at the lower limit and 2 W/cm^2 at the highest excitation. The luminescence radiation was analyzed with a 0.5-m grating spectrometer, with spectral resolution better than 0.3 meV, and detected with a nitrogen-cooled S1 photomultiplier.

D. X-ray diffraction measurements

Cu $k_{\alpha1}$ x-ray rocking curves of the samples for 004 reflection were obtained on a double-crystal system. The experimental setup consists of: microfocus generator (effective focal size of about 50 $\mu m\times50$ μm), a GaAs 004 monochromator and a Lang topographic camera, including an electronic panel and detector. Although steps size in

[This article is copyrighted as indicated in the article. Reuse of AIP content is subject to the terms at: http://scitation.aip.org/termsconditions. Downloaded to] IP: 143.106.108.136 On: Tue, 23 Jun 2015 18:19:15

TABLE I. Physical parameters of the MO sources, growth conditions, and results obtained in bubbling H_2 through a mineral oil bubbler.

MO source	Bath usual temperature (°C)	Physical state at usual temp.	Melting point (°C)	Density (g/cm^3)	Vapor pressure (mm/Hg)	H_2 usual bubbling flow for this work (sccm)	Approximate n of bubbles observed with oil experiments (n/min)	Approximate bubbles volume (cm^3)
TMG	−13	liquid	−15.8	1.10	25	5–10	10 to 14	0.7
TMA	24	liquid	15.4	0.752	11	5–10	8 to 12	0.8
TEG	0	liquid	−82.3	1.057	1.5	90–100	96 to 108	1.0
TMI	18	solid	88	1.568	1.5	75–100	continuous flow	···
TEA	20	liquid	−52	0.835	0.3	···	not utilized	···
TEI	30	liquid	−32	1.260	0.56	···	not utilized	···

θ of the order of 0.1 s of arc can be attained in this system, it has been used at 2 s of arc in the measurements.

IV. RESULTS AND DISCUSSION

A. The simulated bubbling experiment

The MO sources used are commercial 200-g stainless-steel cylinders, equipped with 3.2-mm internal diameter bubbling Teflon deep tube.[22] The number of hydrogen bubbles per minute flowing through the liquid MO source can be estimated by several ways: (a) by using a cylinder transparent source, (b) by calculations using known physical parameters, (c) by simulations using liquids with similar physical properties, (d) by using a microphone and amplifier attached to the cylinder, or (e) by using the MO source in series with a similar transparent low level oil bubbler.[23–25] The last possibility has been chosen and it enables one to count the bubble rate for the same conditions as in the layer growth. The high vapor pressure MO sources like TMG and TMA are manufacturated with a large internal diameter tube as described in Ref. 22. The bubble volume and the MO flow rate depend on the internal deep tube diameter and MO physical parameters.[25] MO parameters and bubbling simulation results are presented in Table I. According to it, high vapor pressure MO like TMG and TMA are transported to the reactor as low flow rate bubbles or pulses. One pulse in the pipe line is generated by a H_2 MO impregnated bubble, inside the cylinder by the Teflon deep tube. The MO pulses are smeared out in travelling the 1.5-m pipe line between MO cylinder and reactor, but it is believed that the MO pulses are not completely diluted within the line. Figure 2 shows a scheme of the TMG cylinder and part of the pipe line. It presents regions of high MO concentration (a pulse) and regions of low MO concentration (the residual part of the pulse).

In order to grow GaAs, $H_2 = 10$ sccm bubbling rate through the TMG cylinder was used and the crystal growth rate is ~ 10 Å/s. Using the simulated low level oil bubbler flow rate, 14 bubbles have been counted per 60 s. Accordingly, one should have ~ 43 Å per bubble or pulse. As to the growth of a 10-Å thin layer, only part of a pulse is necessary. This should explain the nonlinear relationship between layer thickness and growth time observed in very thin layers grown by the APMOVPE technique.[23]

According to the bubble volume and flow rate shown in Table I, it should be better to have cylinders deep bubbling tubes with a smaller diameter than that described in Ref. 22.

The pulse TMA character was overcome by including an orifice within its pipe line, so that the pulse character is restricted to the TMG and TEG MO sources. This means that in the growth of GaAlAs/GaAs and GaInAs/InP, only the gallium sources presents a pulse character. For the H_2 high flow rate MO sources like TEG, the growth rate of GaAs gives ~ 2.7 Å/s and the bubbling simulation gives 1.6 bubbles per s, which implies a better thickness control. Compared to TMG growth one can conclude that it is much more difficult to grow ternary and quaternary layers without composition fluctuation using higher vapor pressure MO sources.

B. Auger characterization of the GaAlAs/GaAs system

Figure 3 shows the AES depth profile of a GaAlAs/GaAs/GaAlAs/substrate sample with nominal thicknesses 500/100/10 000 Å/substrate, Al$\sim$30%, grown using TMG + TMA sources. This structure was grown without

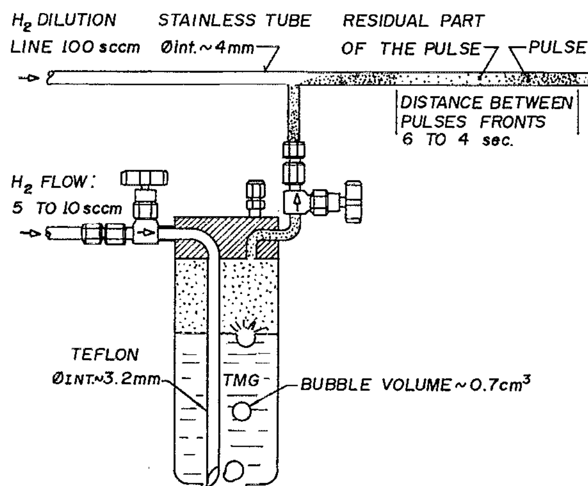

FIG. 2. Representation of the TMG MO source and the pulse flow character the MO vapor is transported to the reactor cell by low flow rate hydrogen carrier gas.

[This article is copyrighted as indicated in the article. Reuse of AIP content is subject to the terms at: http://scitation.aip.org/termsconditions. Downloaded to] IP: 143.106.108.136 On: Tue, 23 Jun 2015 18:19:15

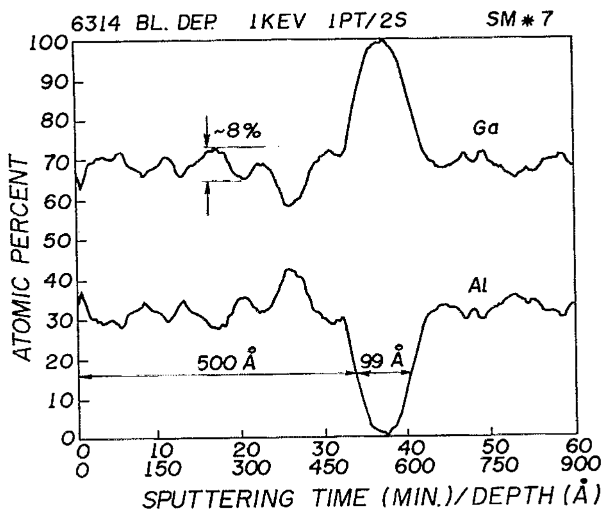

FIG. 3. High-resolution Al and Ga AES depth profile spectra of a GaAlAs/GaAs/GaAlAs (500/100/10000 Å) SQW showing barriers composition fluctuation due to the TMG pulse flow character. The 500-Å barrier growth takes around seven to eight pulses, according to the 30% Al composition growth rate.

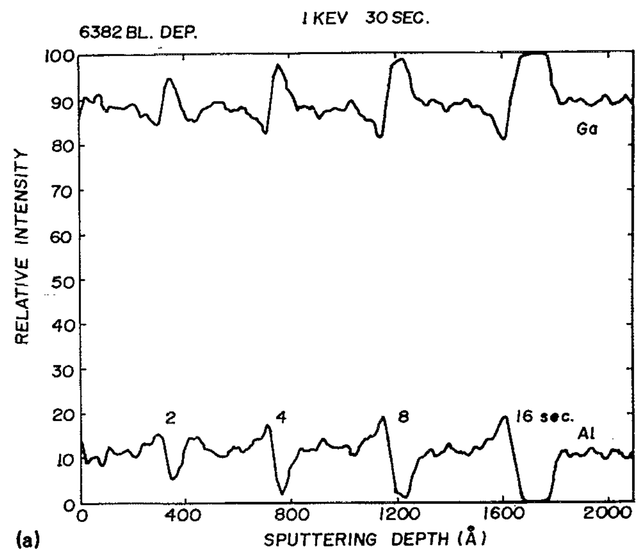

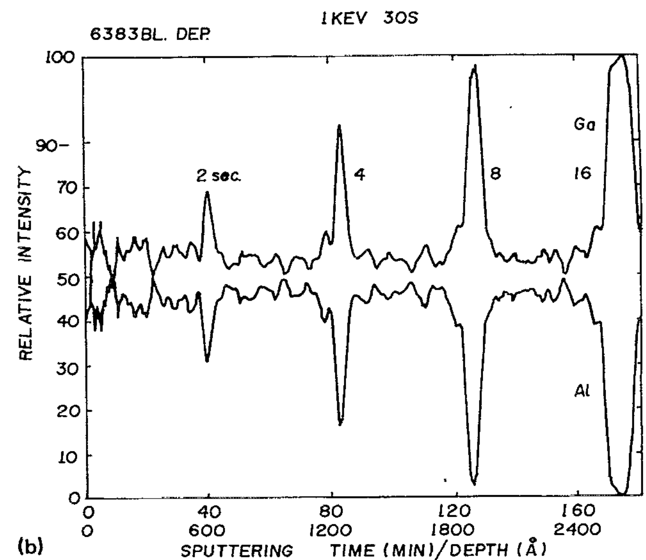

FIG. 4. Al and Ga AES depth profile spectra of 4×GaAlAs/GaAs QWs with 2, 4, 8, and 16 s growth time. (a) Al∼12% and (b) Al∼45%. The Al bumps at the QW interface are due to the pressure imbalance between bypass line and reactor cell. MO sources are TMG + TMA.

stopping the growth at the interfaces. The TMA was directed towards to the bypass line for 10 s during the GaAs SQW construction. From this figure one observes that the ternary barrier has a high composition fluctuation (∼8%) with some periodicity on both sides of the SQW, which is a little disturbed by the TMA flow directed from the bypass to the reactor lines. The higher Al peak observed at the first interface (starting from the surface) is due to a small pressure difference between reactor and bypass lines. Note that the higher Al peak at the interface can disturb the composition fluctuation quasi-periodicity. Similar AES spectra were taken from different regions of the same sample. The growth of the SQW depicted by the AES profile in Fig. 3 takes 10 s and, according to Table I, it should correspond to 2.3 TMG bubbles. The noninteger number of bubbles and the barrier composition fluctuation make it impractical to build a symmetrical and abrupt SQW with these conditions. The left-hand side 500-Å barrier width of Fig. 3 takes 36 s to grow. According to the bubble simulation it should correspond to 7 to 8 TMG pulses, which is approximately the same number of Ga peaks observed.

Figure 4 shows AES depth profiles of multiple GaAlAs/GaAs QW structures, grown with TMG + TMA sources, with the Al average composition of: (a) 12% and (b) 45%. These structures consist of four SQW corresponding to growth time of 2, 4, 8, and 16 s, while the TMA flow was directed to the bypass line. This figure then confirms our conclusions drawn from Fig. 3, and also:

(i) The higher the pressure difference between bypass and reactor lines, the higher the Al peak at the interface [Fig. 4(a)]. This phenomenon has been described by Thrush *et al.* and Sillmon *et al.* and it has been attributed to: vent/run manifold pressure imbalance or gas line impedance or mechanical valve fluctuation.[23,26]

(ii) The lower the Al composition, the lower the amplitude fluctuation. Lower MO composition means lower bubble flow rate. This effect should be due to the fact that at very low bubble flow rate the bubble TMG partial pressure is used to equalize the residual MO pressure of the line. Note that the residual part of the pulse (Fig. 2) and the Venturi effect at the TMG and dilution lines intersection contribute to the growth rate.

(iii) For thinner QW (2, 4, and 8 s growth time) AES depth profiles show Al within the well. The 2 and 4 s QW do not correspond to a whole pulse growth and they could be grown with the residual part of the pulse. This means a QW thinner than the predicted one. The pulse character of the high MO source vapor pressure could also explain striations observed for the growth of GaAlAs.[27] These striations represent lines of different compositions along the growth direction as stated by transmission electron micros-

[This article is copyrighted as indicated in the article. Reuse of AIP content is subject to the terms at: http://scitation.aip.org/termsconditions. Downloaded to] IP: 143.106.108.136 On: Tue, 23 Jun 2015 18:19:15

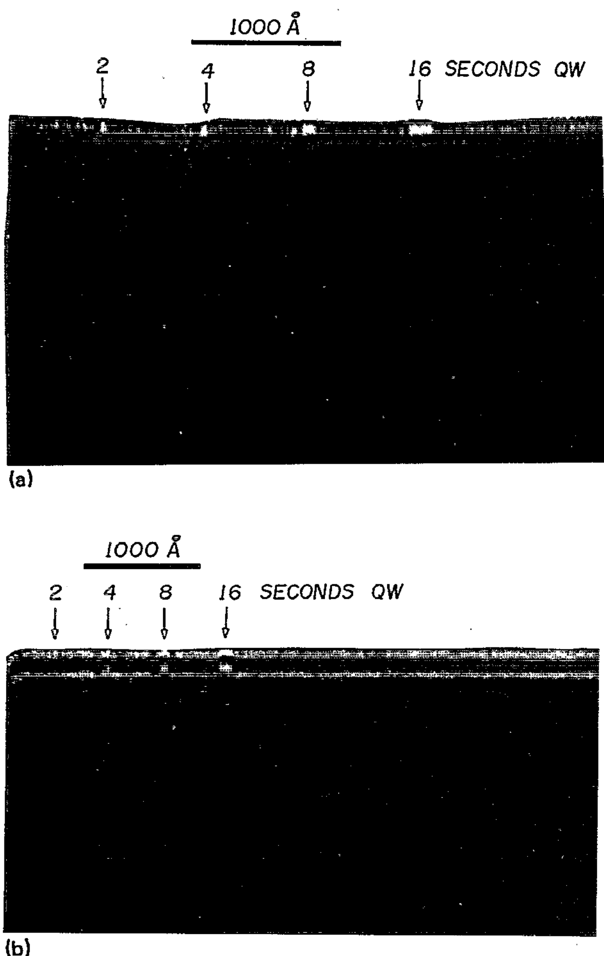

FIG. 5. WTEM pictures of 4×AlGaAs/GaAs QWs heterostructures grown using: (a) TMG + TMA sources, Al% ~45, (b) TEG + TMA sources, Al%~35. The four QWs growth time are 2, 4, 8, 16 s for both cases.

copy described below.

Contrary to the growth using TMG, the AES depth profile of samples grown using TEG + TMA sources, for Al% between 12 and 35, shows the normal 2–3% fluctuation, intrinsic to the AES technique.

C. WTEM characterization of the GaAlAs/GaAs system

Figure 5 shows WTEM pictures of two MQW GaAlAs/GaAs structures: (a) grown using TMG + TMA sources [the same sample as in Fig. (4b)] and (b) grown using TEG + TMA (Al~35%). The QW growth times are the same as for Fig. 4 for both structures. It can be observed that the high degree of QW barrier fluctuation is the case of the TMG source. WTEM spectra of the sample grown using TEG and Al% between 18 and 35 show no barrier fluctuation except at the interface when TMA is turned back to the reactor cell, due to the reactor and bypass lines pressure imbalance.

D. XRD characterization of the GaInAs/InP system

The growth of GaInAs on InP substrates were performed using the combination of TMI + TEG and TMI + TMG flow rates depicted in Table I. For the TMI + TEG case, high quality and purity crystals could be obtained as observed by XRD, SEM, AES, PL, and electrical characterization.[28] The TMI source is solid and the flow is considered as a continuum. By using $H_2 = 75$ sccm through the TMI source one has ~2.5 Å/s for the InP growth rate and $H_2 = 90$ sccm through the TEG source, giving ~2.5 Å/s for the GaAs growth rate. Both TMI + TEG give ~5 Å/s growth rate for the GaInAs (In~53%) growth. According to the crystal quality, both sources can be considered as a continuous flow. This can be observed in Fig. 6(a) which shows the x-ray rocking curve of a GaInAs/InP mismatched heterostructure grown using TMI + TEG sources. The SEM picture of the same etched GaInAs layer and substrate is also shown in this figure.[29]

As to the TMI + TMG case, the ternary layers can be matched only in average to the InP substrate. Figure 6(b) shows the rocking curve of a GaInAs/InP mismatched heterostructure. This figure also shows a SEM picture of the same GaInAs layer and substrate, etched by the ferricyanide technique.[29] The preferential defect etching rate shows the high density of dislocations created during growth. This result is obtained for a GaInAs growth rate between 4 and 7 Å/s. It is supposed that it is due to the low flow rate used in the TMG bubbler, which corresponds to a high growth rate per bubble. The average lattice mismatch, obtained from the rocking curve [Fig. 6(b)], is $\Delta a/a \sim 2.5 \times 10^{-3}$. The measured half width of half maximum (FWHM) of the layer *RX* rocking curve contribution gives rise to an estimate gallium fluctuation of ΔGa~6%. Note that included in the large FWHM are: the effect of TMG source fluctuation, defects, and alloy broadening. Smeets and Cox[30] also found that the FWHM in their XRD result for the TMI + TMG case is larger than that for TMI + TEG. They proposed that this is due to a small difference of pressure between run/vent lines in growing GaInAs on InP. Here, it is proposed by an explanation based on the pulse character of the TMG source instead. In order to match ternary and quaternary layers one can either use low vapor pressure MO sources, depicted in Table I or the adducts proposed by Moss.[31] Therefore the ethyl and adduct MO groups still have some problems concerning source purity. Alternate solutions like: needdle valves or capilarity, mixing chamber or simply discarding part of the MO by bubbling a high H_2 flow rate, are proposed to overcome the pulsed MO character.[30,32,33] One believes that one of the most satisfactory solutions for APMOVPE is the use of the better purity methyl MO group and the use of the diffuser system proposed by Mircea *et al.* The diffuser solution uses hydrogen flow rates of ~1000 sccm for TMI and ~100 sccm for TMG without bubbling.[34]

E. Optical characterization

Figure 7 shows the PL spectra of the four AlGaAs/GaAs QWs (TMG + TMA) presented in Fig. 4(a) at 77

[This article is copyrighted as indicated in the article. Reuse of AIP content is subject to the terms at: http://scitation.aip.org/termsconditions. Downloaded to] IP: 143.106.108.136 On: Tue, 23 Jun 2015 18:19:15

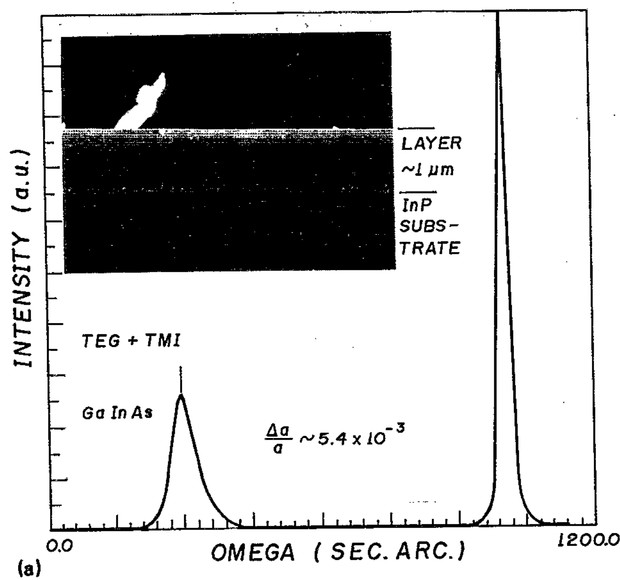

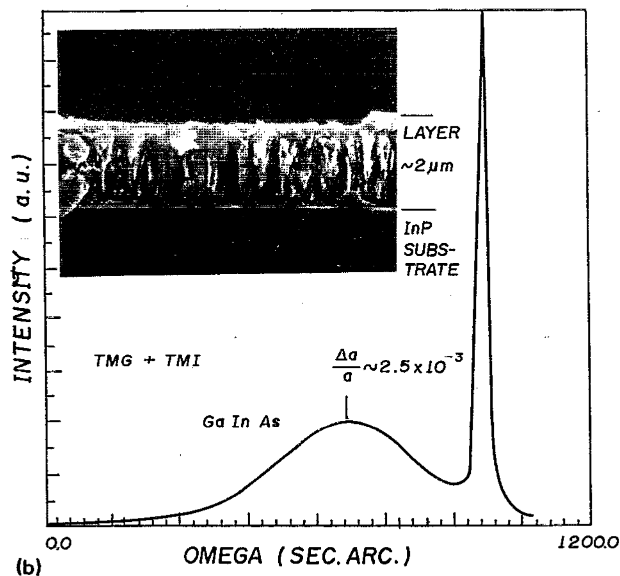

FIG. 6. XRD rocking curve of 004 GaInAs layers grown on InP substrate using Cu $k_{\alpha 1}$ radiation: (a) MO sources are TEG + TMI. The layer and substrate mismatch is $\Delta a/a \sim 5.4 \times 10^{-3}$. The SEM picture shows the same ferricyanide etched GaInAs/InP structure with relatively clean cleavage plane. (b) MO sources are TMG + TMI. The FWHM of the GaInAs layer corresponds to ~6% Ga composition fluctuation. The layer and substrate average mismatch is $\Delta a/a \sim 2.5 \times 10^{-3}$. The SEM picture shows the same ferricyanide etched GaInAs/InP structure with a high density of defects.

and 2 K. At 2 K only peaks due to recombination of the free exciton associated with the electron and the heavy-hole first subbands (1 H) are observable. At 77 K it is also observed that a small peak is related to the free exciton involving the light-hole ground state (1 L). The disappearence of the (1 L) emission at 2 K is due to the depletion of the light-hole sub-band population. Since the (1 L)-(1 H) splitting decreases as the well thickness increases, the (1 L) emission is clearly observable for thinner

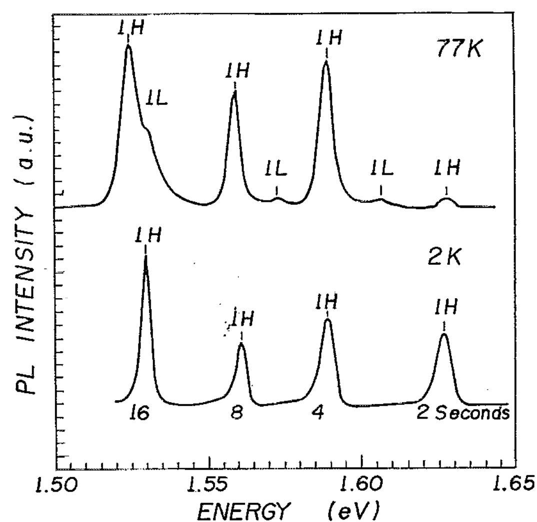

FIG. 7. PL spectra of the structure shown in Fig. 4(a) and grown using TMG + TMA sources. The Al% is 12 and the four QWs growth time are 2, 4, 8, and 16 s. The linewitdths are between 3.3 and 5.9 meV (see Fig. 8). H and L correspond to $e \rightarrow$heavy and light holes transitions, respectively.

wells but becomes unresolved for the wider ones.[7-10] The calculated transition energies considering square wells widths values, obtained by AES, agrees within a reasonable error with the measured PL lines. The measured PL linewidths (3.3–5.9 meV, see Fig. 8) are considered as an indication of good quality samples, comparable to the best MOVPE results. Samples grown by this technique usually exhibit unresolved excitonic spectra, consisting of a single peak with linewidth ranging from 4 to 10 meV.[11-13,35-38] In the case of MBE samples, the PL spectra of SQW structures consist of resolved free and bound exciton lines with much narrow linewidths (as narrow as 0.15 meV).[7-10]

It should be pointed out that the PL linewidths shown in Fig. 7 actually decrease from 2 to 77 K. This unusual behavior is probably due to the recombination of both free

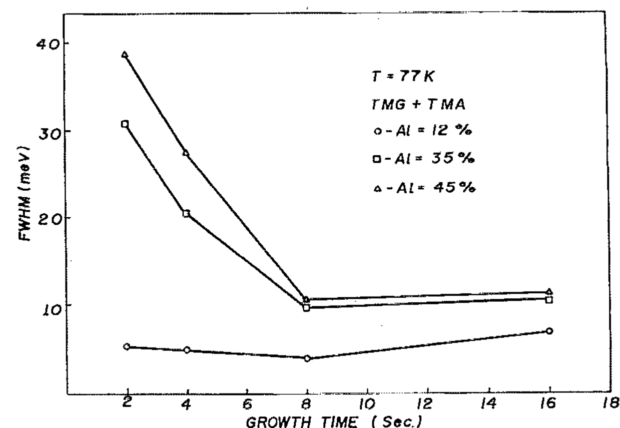

FIG. 8. PL linewidth (FWHM) vs QWs growth time for different Al barriers composition for TMG + TMA sources. The GaAs QW growth rate, extracted from thick layer, is 10 Å/s. Note that the higher the Al% the higher the FWHM value.

[This article is copyrighted as indicated in the article. Reuse of AIP content is subject to the terms at: http://scitation.aip.org/termsconditions. Downloaded to] IP: 143.106.108.136 On: Tue, 23 Jun 2015 18:19:15

and bound excitons at 2 K, which are not resolved in our spectra, but contribute to broaden the low-energy side of the 2 K lines. At 77 K it does not occur since the bound excitons are already thermalized. Figure 8 shows PL linewidth as a function of the growth time. We observe that the usual broadening as the QW thickness is decreased.[35–38] In Fig. 8 is depicted a less explored aspect of the PL linewidth and its dependence on the alloy composition of the barrier layer. One observes that the PL linewidth increases with the aluminum composition of the barrier layer, and that this dependence is more remarkable for a thinner QW. The usual PL linewidth analysis consists of comparing the measured values with the variation of the energy levels due to well width fluctuations.[11–13,35–38] Using this model, the sample shown in Fig. 7 exhibits, however, linewidths smaller than the calculated values, corresponding to 1 monolayer fluctuation.[11–13] This simple model cannot explain either the better MBE results or the observed dependence of the alloy composition in the barrier. One proposes two possible effects to explain the observed PL linewidth behavior, based on more accurate models developed by Ogale *et al.*[39] and Welch *et al.*:[40] (i) the broadening is related to the sub-band filling by high carrier concentration and is originated from unintentional donors in the barrier.[40] The donor concentration in MOVPE samples (intrinsic n type) is probably higher than in MBE samples (normally intrinsic p type), and increases with aluminum composition as mentioned in Sec. II B; (ii) Ogale *et al.*[39] demonstrated that the PL linewidth increases with aluminum composition on the barrier layer and that this dependence increases significantly for high composition fluctuation of the barrier ternary compound. This is in agreement with our conclusions that high vapor pressure MOVPE samples exhibit a high fluctuation of ternary composition, as compared to MBE samples and that the fluctuation increases with the aluminum composition. PL measurements at 2 K were performed on the sample grown using (TEG + TMA sources), changing the power excitation from 0.1 to 2.0 W/cm^2. As can be observed in Fig. 9 the spectra show significant contribution due to bound exciton transitions (lower energy side of each peak). These PL peaks correspond to 8 and 16 s growth time AlGaAs/GaAs QW, for Al$\sim$18%. The broad bound exciton region observed in Fig. 9 is probably due to more than one impurity level. The intrinsic impurity level for this case is $n \sim 1 \times 10^{16}$ cm^{-3}, which is much higher than that for the sample shown in Fig. 7 ($n \sim 6 \times 10^{14}$ cm^{-3}). It is then concluded that: (i) QW linewidth broadening for Fig. 7 is due mainly to the barrier Al fluctuation. For high Al% the broadening can also be dominated by the higher intrinsic doping level (TMG + TMA sources), (ii) the linewidth broadening for Fig. 9 is dominated mainly by the high intrinsic doping level (TEG + TMA sources).

V. CONCLUSIONS

The APMOVPE technique is used to grow GaAlAs/GaAs and GaInAs/InP thin and thick layer heterostructures, using high TMG and low TEG vapor pressure MO sources. AES, WTEM, XRD, and low temperature PL spectroscopy were used to characterize these MOVPE heterostructures. AES, WTEM, and XRD techniques show a high degree of ternary alloy composition fluctuation. PL technique shows that even having composition fluctuation, one can obtain high quality QW samples with low Al content. It is proposed that the ternary composition fluctuation is due to the pulse character of the MO molecules transported to the reaction chamber and that the nonuniformity is an intrinsic consequence of the bubbler method for extracting the MO from their cylinders. The pulse character was confirmed by bubbling simulations which gives tens of Å growth rate per pulse for high vapor pressure TMG source and few Å growth rate per pulse for low vapor pressure TEG source. The pulse MO growth character can provide explanations for some nonexplained problems: nonlinearity between layer thickness and growth time observed for thin layers and layers striations along the growth direction. Finally the solutions reported in the literature to overcome the high vapor pressure MO source pulse character are discussed.

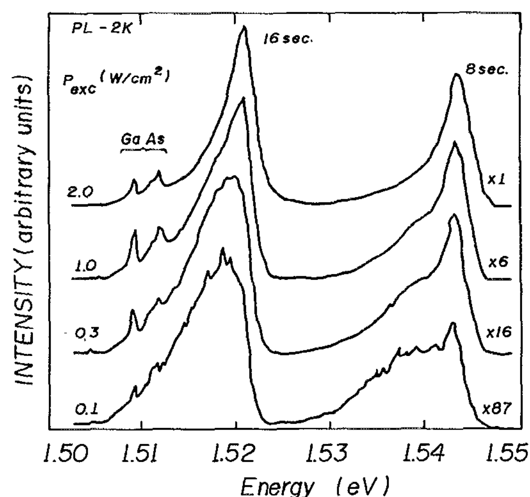

FIG. 9. 2 K PL spectra showing the bound and free exciton regions behavior with the excitation power for 8 and 16 s QWs growth time. The growth was performed with TEG + TMA (Al$\sim$18%) sources. Note that the 16 s QW is also broadened by the GaAs excitonic transitions.

ACKNOWLEDGMENTS

The authors wish to thank A. Bernussi, M. Furtado, and B. Waldman for critical reading of the manuscript and M. Pollo, H. Bertan, and H. Campos for technical assistance in preparing this work.

[1] T. Fukui, H. Saito, and Y. Tohara, Jpn. J. Appl. Phys. **27**, L1320 (1988).
[2] J. Gaines, P. Petroff, and J. English, J. Vac. Sci. Technol. B **6**, 1378 (1988).
[3] M. Leys, C. Opdorp, M. Viegers, and H. Mecheen, J. Cryst. Growth **68**, 431 (1984).
[4] L. Esaki, IEEE J. Quantum Electron. **QE-22**, 1611 (1986).
[5] J. English, A. Gossard, H. Stomer, and K. Baldwin, Appl. Phys. Lett. **50**, 1826 (1987).
[6] M. Shayegan, V. Goldman, C. Jiang, T. Sajoto, and M. Santos, Appl. Phys. Lett. **52**, 1086 (1988).
[7] Y. Chen, E. Koteles, J. Lee, J. Chi, and B. Elman, Proceed. SPIE,

[This article is copyrighted as indicated in the article. Reuse of AIP content is subject to the terms at: http://scitation.aip.org/termsconditions. Downloaded to] IP: 143.106.108.136 On: Tue, 23 Jun 2015 18:19:15

Quantum Well and Superlattices Physics **792**, 162 (1987).
[8] B. Deveaud, A. Regreny, J. Emery, and A. Chomette, J. Appl. Phys. **59**, 1633 (1986).
[9] C. Tu, R. Miller, B. Wilson, P. Petroff, T. Harris, R. Kopt, S. Sputz, and M. Lamont, J. Cryst. Growth **81**, 159 (1987).
[10] R. Tsui, G. Kramer, J. Curless, and M. Peffley, Appl. Phys. Lett. **48**, 940 (1986).
[11] T. Kuech, E. Veuhoff, T. Kuan, V. Deline, and R. Potenski, J. Cryst. Growth 77, 257 (1986).
[12] D. Bertolet, J. Knei, and K. Lau, J. Appl. Phys. **62**, 120 (1987).
[13] P. Frijlink, J. Cryst. Growth **93**, 207 (1988).
[14] M. Razeghi, F. Omnes, J. Nagle, and P. Bove, Appl. Phys. Lett. **55**, 1677 (1989).
[15] D. Nicholas, A. Peaker, E. Thrush, and J. Davis, Inst. Phys. Conf. Ser. *n*° 91, 295 (1987).
[16] G. Laube, U. Kohler, and J. Weidlen, J. Cryst. Growth **93**, 45 (1988).
[17] J. Cunningham, T. Chiu, G. Timp, E. Aggekum, and W. Tsang, Appl. Phys. Lett. **53**, 1285 (1988).
[18] Y. Kawagachi, H. Asahi, and H. Nagai, Inst. Phys. Conf. Ser. *n*° 79, 79 (1986).
[19] W. Tsang, A. Chang, and J. Ditzenberger, Appl. Phys. Lett. **49**, 960 (1986).
[20] J. Faist, J. D. Ganière, P. Buffat, S. Sampson, and F. R. Reinhart, J. Appl. Phys. **66**, 1023 (1989).
[21] J. D. Ganière, F. Reinhart, R. Spycher, B. Bourqui, A. Catana, P. Ruterana, P. Stadelmann, and P. Buffat, J. Microsc. Spectrosc. Electron. **14**, 407 (1989).
[22] Alfa Ventron Catalogue (1986).
[23] E. Thrush, J. Whiteaway, G. Evans, D. Wight, and A. Cullis, J. Cryst. Growth **68**, 412 (1984).
[24] S. Hersee and J. Ballingall, J. Vac. Sci. Technol. A **8**, 800 (1990).
[25] H. Boeglin, L. Kenney, and P. Rhodes, Microelectronic Manufacturing and Testing **13**, 23 (1990).
[26] R. Sillmon, N. Bottka, J. Butler, and D. Gaskill, J. Cryst. Growth **77**, 73 (1986).
[27] C. Schaus, J. Shealy, and L. Eastman, J. Appl. Phys. **59**, 678 (1986).
[28] M. Sacilotti and A. C. Bordeaux Rego, Revista Brasileira de Física Aplicada e Instrumentação **4**, 189 (1989).
[29] R. Chow and Y. Chai, Appl. Phys. Lett. **42**, 383 (1983).
[30] E. Smeets and A. Cox, J. Cryst. Growth **77**, 347 (1986).
[31] R. Moss, J. Cryst. Growth **68**, 78 (1984).
[32] M. Razeghi, M. Poisson, J. Larivain, and J. Duchemin, J. Electron. Mater. **12**, 371 (1983).
[33] C. Chang, Y. Su, M. Lee, L. Chen, and M. Houng, J. Cryst. Growth **55**, 24 (1981).
[34] A. Mircea, R. Mellet, B. Rose, P. Dasté, and G. Schiavini, J. Cryst. Growth **77**, 340 (1986).
[35] M. Tanaka, H. Sasaki, J. Yoshino, and T. Furuta, Surf. Science **174**, 65 (1986).
[36] H. Kawai, K. Kaneko, and N. Watanabe, J. Appl. Phys. **56**, 463 (1984).
[37] H. Sasaki, M. Tanaka, and J. Yoshino, Jpn. J. Appl. Phys. **24**, L417 (1985).
[38] M. Tanaka and H. Sasaki, J. Cryst. Growth **81**, 153 (1987).
[39] S. Ogale, A. Madhukar, F. Voillot, M. Thomsen, W. Tang, T. Lee, J. Kim, and P. Chen, Phys. Rev. B **36**, 1662 (1987).
[40] D. Welch, G. Wicks, and L. Eastman, Appl. Phys. Lett. **46**, 991 (1985).

[This article is copyrighted as indicated in the article. Reuse of AIP content is subject to the terms at: http://scitation.aip.org/termsconditions. Downloaded to] IP: 143.106.108.136 On: Tue, 23 Jun 2015 18:19:15